

# Repulsive lateral van der Waals force

Edson C. M. Nogueira,<sup>1,\*</sup> Lucas Queiroz,<sup>1,†</sup> and Danilo T. Alves<sup>1,‡</sup>

<sup>1</sup>*Faculdade de Física, Universidade Federal do Pará, 66075-110, Belém, Pará, Brazil*

(Dated: October 26, 2021)

In the literature, it has been shown that between a neutral polarizable particle and a conducting plane surface arises an attractive dispersive force. A change on this geometry, for instance by the presence of a hole, can be felt by an anisotropic particle as a repulsive force, normal to the surface. In the present paper, we introduce a single slight protuberance, with a certain characteristic width, in the geometry of a perfectly conducting plane, and show that, beyond a correction to the normal attractive force already present in the absence of the protuberance, a neutral anisotropic polarizable particle feels a lateral van der Waals force which, under certain circumstances, repels it towards points that are several widths distant from the center of the protuberance. Moreover, we show that a similar repulsive effect arises in the classical context, involving a neutral particle with a permanent dipole moment.

In 1873, van der Waals proposed an equation of state for real gases, which included a term related to intermolecular attractive forces [1]. For the case of two non-polar molecules, the intermolecular forces, usually called dispersion van der Waals (vdW) forces, are due to the quantum fluctuations in the distributions of charges and currents in these molecules [2, 3]. The influence of retardation effects, related to the speed of light, on these dispersive forces is obtained in the context of the quantum electrodynamics [4–6]. Dispersive forces are also related, for instance, to the attraction between two perfectly conducting parallel plates [7], and between a neutral polarizable particle and a conducting plane surface [7, 8]. In general, dispersive forces depend on the material properties and on the geometry of the material bodies involved [9–16], and the progress in the precision of the experiments has opened possibilities for applications in micro and nanotechnology [17–20].

The repulsive aspect of the dispersive forces has attracted growing interest [6, 21–38]. For example, a conducting spherical shell experiences an outward repulsive dispersive force [22]. Moreover, there can be repulsion between an electrically polarizable atom and a magnetically polarizable one (or between the correspondent macroscopic bodies) [6, 23–26], between two dielectric bodies separated by a fluid [21, 28], and also between two conducting plates separated by a perfect lens [27]. Anisotropic polarizable particles are fundamental in several situations of repulsive dispersive forces [29, 30, 34, 35, 39]. For example, an anisotropic particle can feel a normal repulsive force when put on the symmetry axis of a thin metal plate with a hole [29] [see Fig. 1(a.i)], when it is over a perfectly conducting toroid [35] [see Fig. 1(a.ii)], or over an annular disk [39] [see Fig. 1(a.iii)]. In all these examples, when the repulsion occurs, the interaction energy  $U$  has a shape similar to the one illustrated in Fig. 1(a.iv).

When corrugations are considered, lateral forces appear, which can reveal nontrivial geometric effects in dispersive interactions [34, 40–51]. In the present paper, we consider the

geometry of a plane surface ( $z = 0$ ) with a single slight protuberance [as illustrated in Fig. 1(b.I)], and a neutral anisotropic polarizable particle kept constrained to move on the plane  $z = z_0 > 0$ . We show that, for certain particle orientations and characteristic widths of the protuberance, one of the typical dependencies of the vdW interaction energy  $U$  on  $x_0$  is as illustrated in Fig. 1(b.II). Thus, when the particle is over the protuberance, a lateral vdW force repels it to points several widths distant from the protuberance, as illustrated in Fig. 1(b.II). We consider a perfectly conducting surface in the calculations (as done by Casimir and Polder in Ref. [5], and Casimir in Ref. [7]), intending to write simpler formulas, already capable to provide a clear indication of the existence of this repulsive lateral vdW force.

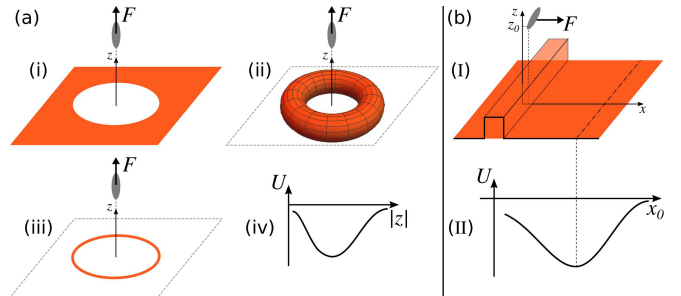


Figure 1. (a) Some examples, from the literature, of configurations [(a.i) – (a.iii)] that produce a *normal* repulsive dispersive force, and their typical common shape of the interaction energy  $U(z)$  (a.iv). (b) One of the examples, discussed in the present paper, of configuration that produces a repulsive *lateral* vdW force (b.I). A single slight protuberance, with a certain characteristic width, is added to a plane. A neutral anisotropic polarizable particle, kept constrained to move on the plane  $z = z_0$ , feels a repulsive lateral vdW force and is pushed to a point several widths distant from the protuberance (b.I). In (b.II), we illustrate one of the typical dependencies of the vdW interaction energy  $U$  on  $x_0$ , found by our calculations.

## I. MODEL AND APPROACH

Let us start considering an anisotropic polarizable particle characterized by a frequency dependent polarizability

\* [edson.moraes.nogueira@icen.ufpa.br](mailto:edson.moraes.nogueira@icen.ufpa.br)

† [lucas.silva@icen.ufpa.br](mailto:lucas.silva@icen.ufpa.br)

‡ [danilo@ufpa.br](mailto:danilo@ufpa.br)

tensor  $\alpha$  given by (see, for instance, Ref. [52])  $\alpha(\omega) = \alpha_1(\omega)\hat{\mathbf{e}}'_1\hat{\mathbf{e}}'_1 + \alpha_2(\omega)\hat{\mathbf{e}}'_2\hat{\mathbf{e}}'_2 + \alpha_3(\omega)\hat{\mathbf{e}}'_3\hat{\mathbf{e}}'_3$ , where  $\hat{\mathbf{e}}'_1$ ,  $\hat{\mathbf{e}}'_2$  and  $\hat{\mathbf{e}}'_3$  are unit vectors pointing in the directions of the principal axes of the particle (see Fig. 2). Denoting the Euler angles by  $(\phi, \theta, \psi)$ , according to the convention usually adopted in quantum mechanics [53, 54], we have  $\hat{\mathbf{e}}'_i = \sum_j R_{ij}\hat{\mathbf{e}}_j$ , where  $R_{ij}$  are the elements of the Euler rotation matrix  $R(\phi, \theta, \psi)$ ,  $\hat{\mathbf{e}}_1 = \hat{\mathbf{x}}$ ,  $\hat{\mathbf{e}}_2 = \hat{\mathbf{y}}$ , and  $\hat{\mathbf{e}}_3 = \hat{\mathbf{z}}$  are unit vectors related to the laboratory coordinate system  $xyz$ , and  $R_{11} = \cos(\theta)\cos(\psi)\cos(\phi) - \sin(\psi)\sin(\phi)$ ,  $R_{12} = -\cos(\theta)\sin(\psi)\cos(\phi) - \cos(\psi)\sin(\phi)$ ,  $R_{13} = \sin(\theta)\cos(\phi)$ ,  $R_{21} = \cos(\theta)\cos(\psi)\sin(\phi) + \sin(\psi)\cos(\phi)$ ,  $R_{22} = \cos(\psi)\cos(\phi) - \cos(\theta)\sin(\psi)\sin(\phi)$ ,  $R_{23} = \sin(\theta)\sin(\phi)$ ,  $R_{31} = -\sin(\theta)\cos(\psi)$ ,  $R_{32} = \sin(\theta)\sin(\psi)$ ,  $R_{33} = \cos(\theta)$ . The particle is located at  $\mathbf{r}_0 = \mathbf{r}_{0\parallel} + z_0\hat{\mathbf{z}}$  (with  $z_0 > 0$  and  $\mathbf{r}_{0\parallel} = x_0\hat{\mathbf{x}} + y_0\hat{\mathbf{y}}$ ), above a grounded conducting corrugated surface described by  $z = h(\mathbf{r}_{\parallel})$ , with  $h(\mathbf{r}_{\parallel})$  describing a general subtle modification [ $\max|h(\mathbf{r}_{\parallel})| = a \ll z'$ ] to a grounded planar conducting surface at  $z = 0$  (see Fig. 2).

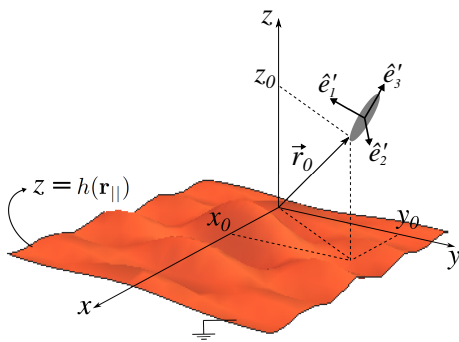


Figure 2. Illustration of a neutral polarizable anisotropic particle, arbitrarily oriented in space, located at  $\mathbf{r}_0 = \mathbf{r}_{0\parallel} + z_0\hat{\mathbf{z}}$  (with  $z_0 > 0$ ), interacting with a general grounded conducting corrugated surface, whose corrugation profile is described by  $z = h(\mathbf{r}_{\parallel})$ . The unit vectors  $\hat{\mathbf{e}}'_1$ ,  $\hat{\mathbf{e}}'_2$  and  $\hat{\mathbf{e}}'_3$  are those pointing to the directions of the principal axes of the particle, in whose directions the particle presents the polarizabilities  $\alpha_1(\omega)$ ,  $\alpha_2(\omega)$ , and  $\alpha_3(\omega)$ , respectively.

To investigate the vdW interaction energy  $U_{\text{vdW}}$  between the particle and the corrugated surface, we take as basis the analytical perturbative approach presented by us in Ref. [51], according to which  $U_{\text{vdW}} \approx U_{\text{vdW}}^{(0)} + U_{\text{vdW}}^{(1)}$ , where  $U_{\text{vdW}}^{(0)}$  is the vdW potential for the case of a grounded conducting plane [8], and  $U_{\text{vdW}}^{(1)}$  (the first-order correction of  $U_{\text{vdW}}^{(0)}$  due to the surface corrugation) is given by  $U_{\text{vdW}}^{(1)}(\mathbf{r}_0) = -\frac{a}{z_0} \sum_{i,j} \mathcal{K}_{ij}(\mathbf{r}_0, h) \int_0^\infty d\xi \alpha_{ij}(i\xi) \hbar / (64\pi^2 \epsilon_0 z_0^3)$  where  $\alpha_{ij}$  are the components of the polarizability tensor in the laboratory system,  $\mathcal{K}_{ij}(\mathbf{r}_0, h) = \frac{1}{a} \int \frac{d^2\mathbf{q}}{(2\pi)^2} \tilde{h}(\mathbf{q}) e^{i\mathbf{q} \cdot \mathbf{r}_{0\parallel}} \mathcal{J}_{ij}(z_0 \mathbf{q})$  are dimensionless functions, and the functions  $\mathcal{J}_{ij} = \mathcal{J}_{ji}$  are

written as

$$\begin{aligned} \mathcal{J}_{xx}(\mathbf{u}) &= \frac{3}{8}|\mathbf{u}|^3 K_3(|\mathbf{u}|) - \frac{3}{8}u_x^2|\mathbf{u}|^2 K_2(|\mathbf{u}|), \\ \mathcal{J}_{yy}(\mathbf{u}) &= \frac{3}{8}|\mathbf{u}|^3 K_3(|\mathbf{u}|) - \frac{3}{8}u_y^2|\mathbf{u}|^2 K_2(|\mathbf{u}|), \\ \mathcal{J}_{zz}(\mathbf{u}) &= \left(2 + \frac{3}{8}|\mathbf{u}|^2\right) |\mathbf{u}|^2 K_2(|\mathbf{u}|) + \frac{1}{4}|\mathbf{u}|^3 K_3(|\mathbf{u}|), \\ \mathcal{J}_{xy}(\mathbf{u}) &= -\frac{3}{8}u_x u_y |\mathbf{u}|^2 K_2(|\mathbf{u}|), \\ \mathcal{J}_{xz}(\mathbf{u}) &= iu_x |\mathbf{u}|^2 K_2(|\mathbf{u}|) - \frac{3i}{8}u_x |\mathbf{u}|^3 K_3(|\mathbf{u}|), \\ \mathcal{J}_{yz}(\mathbf{u}) &= iu_y |\mathbf{u}|^2 K_2(|\mathbf{u}|) - \frac{3i}{8}u_y |\mathbf{u}|^3 K_3(|\mathbf{u}|), \end{aligned}$$

where  $K_2$  and  $K_3$  are modified Bessel functions of the second kind. Note that,  $a/z_0 \ll 1$  is our perturbative parameter,  $\mathcal{K}_{ij}$  are dimensionless functions storing information on the corrugation, and the remaining terms have dimension of energy.

Since we are interested in a particle arbitrarily oriented in space, using the Euler angles we write  $\int_0^\infty d\xi \alpha_{ij}(i\xi) = R(\phi, \theta, \psi) A R^{-1}(\phi, \theta, \psi)$ , where  $A = \int_0^\infty d\xi \text{diag}[\alpha_1(i\xi), \alpha_2(i\xi), \alpha_3(i\xi)]$ . Motivated by the discussion in Ref. [55], we write  $A = \gamma_{\text{iso}} \Pi(\gamma_s, \gamma_a)$  where  $\Pi(\gamma_s, \gamma_a) = I + \gamma_s M_s + \gamma_a M_a$ ,  $I$  is the  $3 \times 3$  identity matrix,  $M_s = \text{diag}(-1, -1, 2)$ ,  $M_a = \text{diag}(-3, 3, 0)$ , and we introduced the parameters  $\gamma_{\text{iso}}$ ,  $\gamma_s$ , and  $\gamma_a$ , which characterize, in a convenient manner, the particle anisotropy, and are given by  $\gamma_{\text{iso}} \equiv \frac{1}{3} \text{Tr}(A)$ ,  $\gamma_s \equiv \frac{1}{3\gamma_{\text{iso}}} [A_{33} - \frac{1}{2}(A_{22} + A_{11})]$ ,  $\gamma_a \equiv \frac{1}{3\gamma_{\text{iso}}} [\frac{1}{2}(A_{22} - A_{11})]$  (assuming the principal axes of the particle have been enumerated in such a way that  $A_{11} \leq A_{22} \leq A_{33}$ ). The  $\gamma$  parameters are such that  $0 \leq \gamma_s < 1$ ,  $0 \leq \gamma_a \leq \min(\gamma_s, 1 - \gamma_s)$ . Note that  $\gamma_s = \gamma_a = 0$  if, and only if, the particle is isotropic. When  $\gamma_s > 0$  and  $\gamma_a = 0$ , one has a class of cylindrically symmetric polarizable particles, of which belongs, for example, a  $\text{CO}_2$  molecule. As  $\gamma_s \rightarrow 1$ , one has  $\gamma_a \rightarrow 0$ , and the polarizability becomes predominant in one of the principal axes of the particle. Taking all this into account, we write

$$\begin{aligned} U_{\text{vdW}}^{(1)}(\mathbf{r}_0; \phi, \theta, \psi) / \mathcal{U}(z_0) &= \\ &- \text{Tr}[\mathcal{K}(\mathbf{r}_0, h) R(\phi, \theta, \psi) \Pi(\gamma_s, \gamma_a) R^{-1}(\phi, \theta, \psi)], \end{aligned} \quad (1)$$

where  $\mathcal{U}(z_0) = \hbar \gamma_{\text{iso}} a / (64\pi^2 \epsilon_0 z_0^4)$ . The dimensionless ratio  $U_{\text{vdW}}^{(1)} / \mathcal{U}(z_0)$  in Eq. (1) is useful to investigate the behavior of the lateral vdW force for a general anisotropic particle, arbitrarily oriented in space, interacting with a perfectly conducting corrugated surface.

## II. APPLICATIONS

We first apply Eq. (1) to investigate the vdW interaction for the situation of a perfectly conducting plane surface with a single slightly protruding strip, as illustrated in Fig. 1(b.I). Specifically, we consider a strip of height  $a$  and width  $d$ , given by  $h(\mathbf{r}_{\parallel}) = a [\Theta(x + \frac{d}{2}) - \Theta(x - \frac{d}{2})]$ , where  $\Theta$  is

the Heaviside step function. For this case, we obtain

$$\mathcal{K}_{ij} = \frac{3}{16} \left[ f_{ij} \left( \frac{x_0}{z_0} + \frac{1}{2} \frac{d}{z_0} \right) - f_{ij} \left( \frac{x_0}{z_0} - \frac{1}{2} \frac{d}{z_0} \right) \right], \quad (2)$$

with

$$\begin{aligned} f_{xx}(u) &= \frac{u^3(8u^4 + 28u^2 + 35)}{(u^2 + 1)^{7/2}}, \\ f_{yy}(u) &= \frac{u(8u^4 + 20u^2 + 15)}{(u^2 + 1)^{5/2}}, \\ f_{zz}(u) &= \frac{u(16u^6 + 56u^4 + 66u^2 + 41)}{(u^2 + 1)^{7/2}}, \\ f_{xz}(u) &= \frac{8u^2 - 7}{(u^2 + 1)^{7/2}}, \\ f_{xy}(u) &= f_{yz}(u) = 0. \end{aligned}$$

As a first case, we consider a particle characterized by  $\gamma_a = 0$  and  $\gamma_s = 0.6$ , kept constrained to move on the plane  $z = z_0$ , and oriented with  $\phi = 0, \theta = \pi/2, \psi = 0$ , which means that  $\hat{e}'_3$  coincides with  $\hat{x}$ . For  $d/z_0 = 0.1$ , the ratio  $U_{\text{vdW}}^{(1)}/\mathcal{U}$  versus  $x_0/z_0$  is shown in Fig. 3. The behavior of  $U_{\text{vdW}}^{(1)}/\mathcal{U}$  reveals the existence of two minimum points at  $x_0/z_0 \approx \pm 0.4$ , and an unstable equilibrium point at  $x_0 = 0$ . Thus, when the particle is slightly dislocated from the position  $x_0 = 0$ , it feels a repulsive lateral vdW force pushing it to distances four times the strip width.

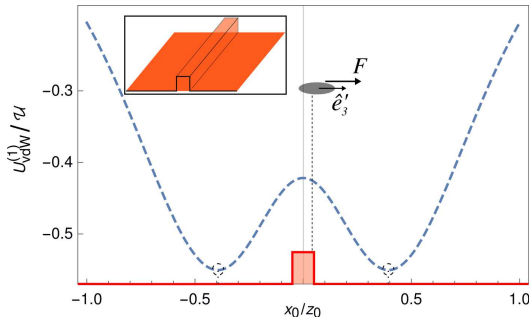


Figure 3. Behavior of the ratio  $U_{\text{vdW}}^{(1)}/\mathcal{U}$  versus  $x_0/z_0$ , for a particle fixed at  $z = z_0$ , and oriented with  $\phi = 0, \theta = \pi/2, \psi = 0$  (in this case, the vector  $\hat{e}'_3$  coincides with  $\hat{x}$ ). The profile of the surface is represented by the solid line, with the single protruding strip with height  $a$  and width  $d$ , being  $d/z_0 = 0.1$  (a 3D visualization is shown in the inset). The repulsive lateral vdW force, indicated by  $F$ , pushes a particle, slightly dislocated from the position  $x_0 = 0$ , to a point distant approximately four times the strip width.

The behavior of  $U_{\text{vdW}}^{(1)}/\mathcal{U}$ , and consequently the existence of a repulsive lateral vdW force, is strongly affected by the particle orientation. For instance, we consider the same particle characterized by  $\gamma_a = 0$  and  $\gamma_s = 0.6$ , oriented with  $\phi = 0, \psi = 0$ , but now considering different values of  $\theta$ , which is shown in Fig. 4. The behavior of  $U_{\text{vdW}}^{(1)}/\mathcal{U}$  for the case  $\theta = 0$  ( $\hat{e}'_3$  coincides with  $\hat{z}$ ), represented by the dotted line in Fig. 4, presents a minimum point at  $x_0 = 0$ . Thus, when the particle is over the strip ( $-d/2 \leq x_0 \leq d/2$ ) and

dislocated from the position  $x_0 = 0$ , it feels an attractive lateral vdW force pulling it back to  $x_0 = 0$ . When  $\theta = \pi/4$  (dot-dashed line), the minimum point,  $x_0 = x_{\min}$ , of  $U_{\text{vdW}}^{(1)}/\mathcal{U}$  is such that  $x_{\min} > d/2$ . This means that when the particle is over the strip it feels a repulsive lateral vdW force, pushing it towards a point distant from the strip. When  $\theta = \pi/2$ , the dashed line shows the same repulsive case already illustrated in Fig. 3. Note that, in this case,  $|x_{\min}|$  is greater than that found for  $\theta = \pi/4$ . Since  $|x_{\min}|$  becomes greater when  $\hat{e}'_3$  coincides with  $\hat{x}$ , hereafter we focus on this orientation.

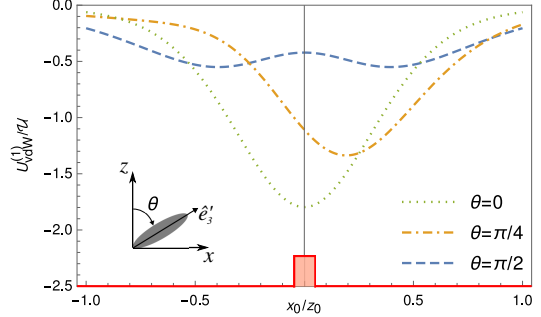


Figure 4. Behavior of the ratio  $U_{\text{vdW}}^{(1)}/\mathcal{U}$  versus  $x_0/z_0$ , for a particle fixed at  $z = z_0$ , characterized by  $\gamma_s = 0.6$ , and oriented with  $\phi = 0, \psi = 0$ , and different values of  $\theta$  (in this case, the vector  $\hat{e}'_3$  is oriented along the  $xz$ -plane). The case  $\theta = 0$ , represented by the dotted line, presents a minimum point at  $x_0 = 0$ , so that one has an attractive lateral vdW force. When  $\theta = \pi/4$  (dot-dashed line), the minimum point is at  $x_{\min} > d/2$ , so that a particle over the strip feels a repulsive lateral vdW force, pushing it towards a point distant from the strip. The case  $\theta = \pi/2$ , represented by the dashed line, shows the same repulsive case already illustrated in Fig. 3; note that  $|x_{\min}|$  for this case is greater than that found for  $\theta = \pi/4$ .

Now, let us investigate how the condition  $|x_{\min}| > d/2$  (which effectively indicates the possibility of existence of a repulsive lateral vdW force) depends on the ratio  $d/z_0$ . Let us use, again, the particle characterized by  $\gamma_a = 0$  and  $\gamma_s = 0.6$ , and oriented with  $\phi = 0, \theta = \pi/2, \psi = 0$ . In Fig. 5, we plot  $x_{\min}/z_0$  as a function of  $d/z_0$ , for  $\gamma_s = 0.6$ , in the dashed line. We highlight the critical value of  $d/z_0$ , called  $(d/z_0)_{\text{crit}}$ , which, in this case, is  $(d/z_0)_{\text{crit}} \approx 0.68$ . One can see that when  $d/z_0 \gtrsim (d/z_0)_{\text{crit}}$ , one has the  $|x_{\min}| < d/2$ , so that the particle is bounded over the strip (attractive lateral vdW force). When  $d/z_0 \lesssim (d/z_0)_{\text{crit}}$ ,  $|x_{\min}| > d/2$ , and we have the particle repelled in relation to the strip (repulsive lateral vdW force). In Fig. 5 it is also shown the behavior of  $x_{\min}/z_0$  versus  $d/z_0$  for other values of  $\gamma_s$ . Note that, as the value of  $\gamma_s$  decreases,  $(d/z_0)_{\text{crit}}$  decreases too, so that the repulsive effect in the lateral vdW force tends to cease.

Since Eq. (1) can be applied to any surface profile, we apply it to other surface geometries to investigate the generality of the repulsive effects discussed so far. For instance, the behavior of the ratio  $U_{\text{vdW}}^{(1)}/\mathcal{U}$  for the case of a Gaussian protuberance, described by  $h(\mathbf{r}_{\parallel}) = ae^{-(r_{\parallel}/d)^2}$ , is shown in Fig. 6(a). As another example, we consider a trapezoidal protuberance, described by  $h(\mathbf{r}_{\parallel}) = a[\Theta(d/2 - |x|) + 2(1 - |x|/d)[\Theta(|x| - d/2) - \Theta(|x| - d)]]$ ,

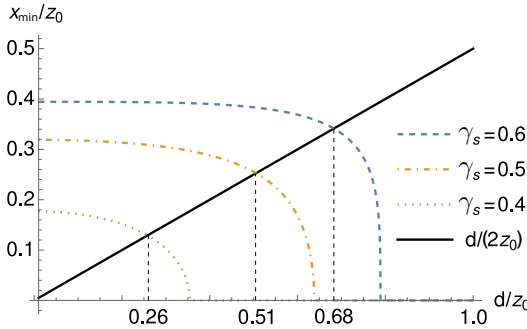


Figure 5. Behavior of  $|x_{\min}|/z_0$  as a function of  $d/z_0$ , for a particle fixed at  $z = z_0$ , oriented with  $\phi = 0, \theta = \pi/2, \psi = 0$ , and characterized by some values of  $\gamma_s$ , namely  $\gamma_s = 0.6$  (dashed curve),  $\gamma_s = 0.5$  (dot-dashed curve), and  $\gamma_s = 0.4$  (dotted curve). The solid line represents  $|x_{\min}| = d/2$  (the repulsive lateral vdW force happens when  $|x_{\min}| > d/2$ ). We highlight some values of  $d/z_0$  correspondent to  $(d/z_0)_{\text{crit}}$ : for  $\gamma = 0.6$ , we have  $(d/z_0)_{\text{crit}} \approx 0.68$  (as discussed in the main text); for  $\gamma = 0.5$ ,  $(d/z_0)_{\text{crit}} \approx 0.51$ ; for  $\gamma = 0.4$ ,  $(d/z_0)_{\text{crit}} \approx 0.26$ .

whose results are shown in Fig. 6(b). Note that in both cases the repulsive lateral vdW force occurs

### III. CLASSICAL CASE

To investigate the existence of lateral repulsive forces in a classical context, involving a neutral particle with a permanent dipole moment  $\mathbf{p}$ , we again take as basis the perturbative approach showed in Ref. [51], according to which the interaction energy  $U_{\text{cla}}$ , between a dipolar particle and a corrugated surface, is given by  $U_{\text{cla}} \approx U_{\text{cla}}^{(0)} + U_{\text{cla}}^{(1)}$ , where  $U_{\text{cla}}^{(0)}$  is the interaction energy for the case of a grounded conducting plane [56], and  $U_{\text{cla}}^{(1)}$  is given by  $U_{\text{cla}}^{(1)}(\mathbf{r}_0) = -\frac{a}{z_0} \sum_{i,j} \mathcal{K}_{ij}(\mathbf{r}_0, h) p_i p_j / (4\pi\epsilon_0 z_0^3)$ . After manipulation of this formula, we obtain

$$U_{\text{cla}}^{(1)}(\mathbf{r}_0; \phi, \theta, \psi) / \mathcal{U}_{\text{cla}}(z_0) = - \text{Tr}[\mathcal{K}(\mathbf{r}_0, h) R(\phi, \theta, \psi) \Pi(1, 0) R^{-1}(\phi, \theta, \psi)], \quad (3)$$

where  $\mathcal{U}_{\text{cla}}(z_0) = a|\mathbf{p}|^2 / (192\pi\epsilon_0 z_0^4)$ . Note that the behavior of the classical ratio  $U_{\text{cla}}^{(1)}(\mathbf{r}_0; \phi, \theta, \psi) / \mathcal{U}_{\text{cla}}(z_0)$  is the same of the quantum ratio  $U_{\text{vdW}}^{(1)}(\mathbf{r}_0; \phi, \theta, \psi) / \mathcal{U}(z_0)$  for  $\gamma_s = 1$ , and  $\gamma_a = 0$ . Therefore, similar repulsive effects also arise in the classical context.

### IV. FINAL REMARKS

From the literature it is known that the particle anisotropy plays a decisive role in the emergence of normal repulsive dispersive forces, as those illustrated in Figs. 1(a.i), (a.ii) and

(a.iii). Here, considering an anisotropic particle, we predict the existence of repulsive lateral vdW forces, as illustrated in Fig. 1(b.I). This repulsive effect is strongly affected by the

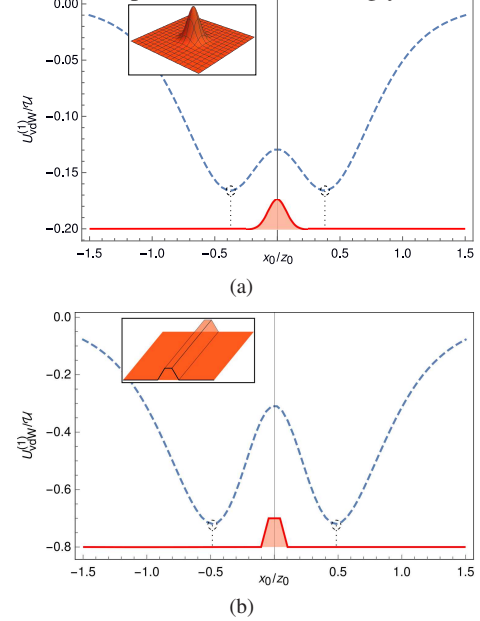


Figure 6. Behavior of the ratio  $U_{\text{vdW}}^{(1)}/\mathcal{U}$  versus  $x_0/z_0$ , for a particle fixed at  $z = z_0$ , and oriented with  $\phi = 0, \theta = \pi/2, \psi = 0$  (in this case, the vector  $\hat{\mathbf{e}}'_3$  coincides with  $\hat{\mathbf{x}}$ ). This behavior is illustrated considering in (a) a single Gaussian protuberance, and in (b) a trapezoidal one, both with  $d/z_0 = 0.1$ . A 2D view of the profiles of these surfaces is represented by the solid lines, whereas 3D visualizations are shown in the insets. Note that in both cases the repulsive lateral vdW force occurs, since we have minimum points of the ratio  $U_{\text{vdW}}^{(1)}/\mathcal{U}$  that are distant from the center of the protuberance.

particle orientation and by the characteristic width of the protuberance introduced on a plane surface. For certain values of these parameters, the particle is pushed towards points that are several widths distant from the center of the protuberance. Moreover, we show that a similar repulsive effect arises in the classical context, involving a neutral particle with a permanent dipole moment. The comprehension of this subtle repulsive aspect in the lateral forces may be relevant to achieve a higher degree of control of the interaction between anisotropic particles near corrugated surfaces, in both quantum and classical domains.

### ACKNOWLEDGMENTS

The authors thank Alexandre Costa, Carlos Farina and Stanley Coelho for valuable discussions. L.Q. and E.C.M.N. were supported by the Coordenação de Aperfeiçoamento de Pessoal de Nível Superior - Brasil (CAPES), Finance Code 001.

---

[1] J. D. van der Waals, *Over de continuiteit van den gas-en vloeistoftostand*, Ph.D. Thesis, Leiden (1873).

[2] R. Eisenschitz and F. London, ber das Verhltens der van der Waalsschen Krfe zu den homopolaren Bindungskrften, *Zeitschrift für Physik* **60**, 491 (1930).

[3] F. London, Zur theorie und systematik der molekularkrften, *Zeitschrift für Physik* **63**, 245 (1930).

[4] H. B. G. Casimir and D. Polder, Influence of Retardation on the London–van der Waals Forces, *Nature* **158**, 787 (1946).

[5] H. B. G. Casimir and D. Polder, The Influence of Retardation on the London–van der Waals Forces, *Phys. Rev.* **73**, 360 (1948).

[6] G. Feinberg and J. Sucher, General theory of the van der Waals interaction: A model-independent approach, *Phys. Rev. A* **2**, 2395 (1970).

[7] H. B. G. Casimir, On the Attraction between Two Perfectly Conducting Plates, *Proc. K. Ned. Akad. Wet.* **B51**, 793 (1948).

[8] J. E. Lennard-Jones, Processes of adsorption and diffusion on solid surfaces, *Trans. Far. Soc.* **28**, 333 (1932).

[9] J. N. Israelachvili, The calculation of van der Waals dispersion forces between macroscopic bodies, *Proceedings of the Royal Society of London. A. Mathematical and Physical Sciences* **205**, 50 (1950).

[10] P. W. Milonni, *The Quantum Vacuum. An Introduction to Quantum Electrodynamics* (Academic Press, San Diego, 1994).

[11] M. Bordag, G. L. Klimchitskaya, U. Mohideen, and V. M. Mostepanenko, *Advances in the Casimir Effect* (Oxford University Press, Oxford, 2009).

[12] J. N. Israelachvili, *Intermolecular and Surface Forces*, 3rd ed. (Academic Press, Amsterdam, 2011).

[13] S. Y. Buhmann, *Dispersion Forces I*, Springer Tracts in Modern Physics, Vol. 247 (Springer Berlin Heidelberg, Berlin, Heidelberg, 2012).

[14] S. Y. Buhmann, *Dispersion Forces II*, Springer Tracts in Modern Physics, Vol. 248 (Springer Berlin Heidelberg, Berlin, Heidelberg, 2012).

[15] R. de Melo e Souza, W. J. M. Kort-Kamp, C. Sigaud, and C. Farina, Image method in the calculation of the van der Waals force between an atom and a conducting surface, *Am. J. Phys.* **81**, 366 (2013).

[16] R. Passante, Dispersion Interactions between Neutral Atoms and the Quantum Electrodynamical Vacuum, *Symmetry* **10**, 735 (2018).

[17] P. Ball, Feel the force, *Nature* **447**, 772 (2007).

[18] A. W. Rodriguez, A. P. McCauley, D. Woolf, F. Capasso, J. D. Joannopoulos, and S. G. Johnson, Nontouching nanoparticle diclusters bound by repulsive and attractive casimir forces, *Phys. Rev. Lett.* **104**, 160402 (2010).

[19] A. W. Rodriguez, F. Capasso, and S. G. Johnson, The Casimir effect in microstructured geometries, *Nature Photonics* **5**, 211 (2011).

[20] M. Keil, O. Amit, S. Zhou, D. Groswasser, Y. Japha, and R. Folman, Fifteen years of cold matter on the atom chip: promise, realizations, and prospects, *J. Mod. Opt.* **63**, 1840 (2016).

[21] I. E. Dzyaloshinskii, E. M. Lifshitz, and L. P. Pitaevskii, General theory of van der Waals' forces, *Soviet Physics Uspekhi* **4**, 153 (1961).

[22] T. H. Boyer, Quantum electromagnetic zero-point energy of a conducting spherical shell and the casimir model for a charged particle, *Phys. Rev.* **174**, 1764 (1968).

[23] T. H. Boyer, Van der Waals forces and zero-point energy for dielectric and permeable materials, *Phys. Rev. A* **9**, 2078 (1974).

[24] D. Kupiszewska, Repulsive Casimir effect, *Journal of Modern Optics* **40**, 517 (1993).

[25] C. Farina, F. C. Santos, and A. C. Tort, On the force between an electrically polarizable atom and a magnetically polarizable one, *Journal of Physics A: Mathematical and General* **35**, 2477 (2002).

[26] C. Farina, F. C. Santos, and A. C. Tort, A simple model for the nonretarded dispersive force between an electrically polarizable atom and a magnetically polarizable one, *American Journal of Physics* **70**, 421 (2002).

[27] U. Leonhardt and T. G. Philbin, Quantum levitation by left-handed metamaterials, *New Journal of Physics* **9**, 254 (2007).

[28] J. N. Munday, F. Capasso, and V. A. Parsegian, Measured long-range repulsive Casimir–Lifshitz forces, *Nature* **457**, 170 (2009).

[29] M. Levin, A. P. McCauley, A. W. Rodriguez, M. T. H. Reid, and S. G. Johnson, Casimir repulsion between metallic objects in vacuum, *Phys. Rev. Lett.* **105**, 090403 (2010).

[30] C. Eberlein and R. Zietal, Casimir–Polder interaction between a polarizable particle and a plate with a hole, *Physical Review A* **83**, 052514 (2011).

[31] K. A. Milton, E. K. Abalo, P. Parashar, N. Pourtolami, I. Brevik, and S. Å. Ellingsen, Repulsive Casimir and Casimir–Polder forces, *Journal of Physics A: Mathematical and Theoretical* **45**, 374006 (2012).

[32] K. V. Shajesh and M. Schaden, Repulsive long-range forces between anisotropic atoms and dielectrics, *Phys. Rev. A* **85**, 012523 (2012).

[33] Y. Hu, R. Sun, Z. Huang, and X. Wu, The repulsive Casimir force with metallic ellipsoid structure, *Journal of Nanotechnology* **2016** (2016).

[34] S. Y. Buhmann, V. N. Marachevsky, and S. Scheel, Impact of anisotropy on the interaction of an atom with a one-dimensional nano-grating, *Int. J. Mod. Phys. A* **31**, 1641029 (2016).

[35] P. P. Abrantes, Y. França, F. S. S. da Rosa, C. Farina, and R. de Melo e Souza, Repulsive van der Waals interaction between a quantum particle and a conducting toroid, *Phys. Rev. A* **98**, 012511 (2018).

[36] K. Sinha, Repulsive vacuum-induced forces on a magnetic particle, *Phys. Rev. A* **97**, 032513 (2018).

[37] P. S. Venkataram, S. Molesky, P. Chao, and A. W. Rodriguez, Fundamental limits to attractive and repulsive Casimir–Polder forces, *Phys. Rev. A* **101**, 052115 (2020).

[38] M. F. Maghrebi, Diagrammatic expansion of the Casimir energy in multiple reflections: Theory and applications, *Physical Review D* **83**, 045004 (2011).

[39] J. J. Marchetta, P. Parashar, and K. V. Shajesh, Geometrical dependence in Casimir–Polder repulsion, *Phys. Rev. A* **104**, 032209 (2021).

[40] V. B. Bezerra, G. L. Klimchitskaya, and C. Romero, Surface roughness contribution to the Casimir interaction between an isolated atom and a cavity wall, *Phys. Rev. A* **61**, 022115 (2000).

[41] D. A. R. Dalvit, P. A. M. Neto, A. Lambrecht, and S. Reynaud, Probing Quantum-Vacuum Geometrical Effects with Cold Atoms, *Phys. Rev. Lett.* **100**, 040405 (2008).

[42] D. A. R. Dalvit, P. A. M. Neto, A. Lambrecht, and S. Reynaud, Lateral Casimir–Polder force with corrugated surfaces, *Journal of Physics A: Mathematical and Theoretical* **41**, 164028 (2008).

[43] B. Döbrich, M. DeKieviet, and H. Gies, Scalar Casimir–Polder forces for uniaxial corrugations,

*Phys. Rev. D* **78**, 125022 (2008).

[44] R. Messina, D. A. R. Dalvit, P. A. M. Neto, A. Lambrecht, and S. Reynaud, Dispersive interactions between atoms and nonplanar surfaces, *Physical Review A* **80**, 022119 (2009).

[45] G. A. Moreno, D. A. R. Dalvit, and E. Calzetta, Bragg spectroscopy for measuring Casimir–Polder interactions with Bose–Einstein condensates above corrugated surfaces, *New Journal of Physics* **12**, 033009 (2010).

[46] A. M. Contreras-Reyes, R. Guérout, P. A. M. Neto, D. A. R. Dalvit, A. Lambrecht, and S. Reynaud, Casimir–Polder interaction between an atom and a dielectric grating, *Physical Review A* **82**, 052517 (2010).

[47] G. A. Moreno, R. Messina, D. A. R. Dalvit, A. Lambrecht, P. A. Maia Neto, and S. Reynaud, Disorder in Quantum Vacuum: Casimir-Induced Localization of Matter Waves, *Physical Review Letters* **105**, 210401 (2010).

[48] G. Bimonte, T. Emig, and M. Kardar, Casimir–Polder interaction for gently curved surfaces, *Physical Review D* **90**, 081702 (2014).

[49] V. Marachevsky, Fluctuation potential of the interaction between a neutral atom and a diffraction grating., *Theoretical & Mathematical Physics* **185** (2015).

[50] R. Bennett, Spontaneous decay rate and Casimir–Polder potential of an atom near a lithographed surface, *Phys. Rev. A* **92**, 022503 (2015).

[51] E. C. M. Nogueira, L. Queiroz, and D. T. Alves, Peak, valley, and intermediate regimes in the lateral van der Waals force, *Phys. Rev. A* **104**, 012816 (2021).

[52] P. Thiyam, P. Parashar, K. V. Shajesh, C. Persson, M. Schaden, I. Brevik, D. F. Parsons, K. A. Milton, O. I. Malyi, and M. Boström, Anisotropic contribution to the van der Waals and the Casimir–Polder energies for  $CO_2$  and  $CH_4$  molecules near surfaces and thin films, *Phys. Rev. A* **92**, 052704 (2015).

[53] J. J. Sakurai, *Modern quantum mechanics; rev. ed.* (Addison-Wesley, Reading, MA, 1994).

[54] L. E. Ballentine, *Quantum mechanics: a modern development; 2nd ed.* (World Scientific, Hackensack, NJ, 2014).

[55] M. Lewis, Z. Wu, and R. Glaser, Polarizabilities of carbon dioxide and carbodiimide. assessment of theoretical model dependencies on dipole polarizabilities and dipole polarizability anisotropies, *The Journal of Physical Chemistry A* **104**, 11355 (2000), <https://doi.org/10.1021/jp002927r>.

[56] J. D. Jackson, *Classical Electrodynamics*, 3rd ed. (Wiley, 1998).